An Experimentally Verified Theoretical Study Of the Falling Cylinder Viscometer

JOHN LOHRENZ, G. W. SWIFT, and FRED KURATA

University of Kansas, Lawrence, Kansas

A theoretical analysis was made for laminar fluid flow in the annulus of a falling cylinder viscometer. A viscometer calibration constant was defined from the results of this analysis. This constant was expressed in terms of only the physical dimensions of the viscometer. The validity of the theory was demonstrated by the agreement between predicted and experimental values of the viscometer constant.

Methods of representing calibration data were compared. Temperature and pressure effects on the viscometer constants were related to the mechanical properties of the viscometer materials.

The results of this investigation showed that the practical design of falling cyclinder viscometers is possible.

Falling and rolling ball viscometer viscometers have been widely used in this country, while the falling cylinder viscometer has received little attention. The ball viscometer has disadvantages which can be overcome when a cylinder is used. First, the motion of the ball during its descent in the viscometer tube exhibits random slip and spin. On the other hand the cylinder, when equipped with stabilizing projections, shows little if any tendency toward dissipating energy in this fashion. Thus the error in measuring experimental fall times is reduced. Second, when ball viscometers are used for measuring low viscosities, the ball diameter must be nearly equal to the tube diameter, making the instrument extremely sensitive to the effects of nonuniform construction. Poor reproducibility results. The cylinder however may be easily oriented in a consistent fashion so that any effect of nonuniform construction is constant.

The theory of the ball viscometer has been extensively treated; one of the better known works being that of Hubbard and Brown (2) who used dimensional analysis to develop a rather satisfactory method for designing a ball viscometer. On the other hand the theory of the falling cylinder viscometer has not fully been exploited.

In the region where Stokes' law applies the analyses (1) for cylinder and ball viscometers lead to

$$\mu \propto \frac{(\sigma - \rho)}{v}$$

If the velocity is measured by determining the fall time interval between two fiducial marks a constant distance apart, a viscometer constant is defined by

$$\beta = \frac{\mu}{(\sigma - \rho)\theta} \qquad (1)$$

To predict the viscometer constant from Stokes' law an empirical correction for the wall effect would have to be introduced. For falling cylinder viscometers a more rigorous approach would consider the fluid flowing in an annulus with appropriate boundary conditions. This approach is similar to that of Lawaczeck (1); however he assumed the annulus could be approximated by the geometry of parallel plates.

THEORETICAL ANALYSIS

Consider a vertical tube of radius R_2 filled with a homogeneous fluid of constant density. A body with a major radius R_1 ($R_2 > R_1$) and total volume V is falling inside a tube at a terminal velocity. The body is oriented parallel and concentric to the center line of the tube. Both the tube and the body are smooth.

The fluid in the tube is Newtonian. Assume perfectly laminar flow with a fully developed flow profile for a distance l along the body. Equating pressure and shear forces for a general cylindrical shell of fluid between tube and body one gets

$$\pi(r^2 - r^2_{max})\,\Delta P_{1st} = -2\pi r l \tau \qquad (2)$$

From the definition of Newtonian viscosity

$$\tau = \frac{\mu}{g_c}\left(\frac{du}{dr}\right) \qquad (3)$$

Substituting Equation (3) into Equation (2) and using the boundary conditions one obtains

$$\text{at } r = R_2,\ u = 0,$$

$$\text{at } r = R_1,\ u = -v$$

Integration yields the following equation:

$$u = \frac{g_c \Delta P_{1st}}{2\mu l}\left[\frac{R_2^2 - r^2}{2} + \left(\frac{\frac{2\mu l v}{g_c \Delta P_{1st}} + \frac{R_2^2 - R_1^2}{2}}{\ln \frac{R_2}{R_1}}\right)\ln \frac{r}{R_2}\right] \qquad (4)$$

Figure 1 shows the flow profile and shear diagram defined by Equations (3) and (4).

The volumetric flow rate is related to the point fluid velocity and terminal velocity of the body as follows:

$$Q = \int_{R_1}^{R_2} 2\pi r u \cdot dr = v\pi R_1^2 \qquad (5)$$

Substituting Equation (4) into Equation (5), integrating, and rearranging one gets

$$\Delta P_{1st} = \frac{4\mu l v}{g_c[(R_2^2 + R_1^2)\ln(R_2/R_1) - (R_2^2 - R_1^2)]} \qquad (6)$$

The force of gravity on the falling body at the terminal velocity is exactly balanced by the following forces:

1. Skin friction along the body and the force due to the pressure difference along the body.
2. Contraction friction at the leading face of the body.
3. Expansion friction at the trailing edge of the body.
4. Friction due to imperfections in the system geometry, for example eccentricity and/or imperfections on the surface of the body and tube.

John Lohrenz and G. W. Swift are with the Continental Oil Company, Ponca City, Oklahoma.

If contraction, expansion, and imperfections effects are negligible, and flow is perfectly laminar, the force of gravity is equal to the forces due to skin friction and the pressure difference on the body. The force due to skin friction may be found by differentiating Equation (4) with respect to r, setting r equal to R_1, substituting in Equation (3), and multiplying by $2\pi R_1$. The forces due to gravity and the pressure difference on the body may be easily written and included in the general force balance:

$$F_g = V(\sigma-\rho)\frac{g}{g_c} = \frac{\pi R_1^2 \Delta P_{1sf}}{16} + \frac{\Delta P_{1sf}}{2}\left[2\left[\frac{\frac{2l\mu v}{g_c \Delta P_{1sf}} + \frac{R_2^2-R_1^2}{32}}{\ln\frac{R_2}{R_1}}\right] - \frac{R_1^2}{8}\right] \quad (7)$$

Substitution of Equation (6) into Equation (7) yields, after rearrangement

$$\beta_{1sf} = \frac{1' g D_e^2}{16 sl} \quad (8)$$

β_{1sf} is equal to β when only laminar flow friction occurs in the viscometer. Because of uncertainty of the assumption of laminar flow and the difficulty in measuring the pertinent dimensions with sufficient accuracy β is determined by calibration with fluids of known viscosity, while β_{1sf} is defined by the use of the physical dimensions of the viscometer.

EXPERIMENTAL WORK

The experimental calibration data used were those previously reported by Swift. (*4*). The experimental apparatus and procedure and the six different falling bodies used have been described by Swift et al. (*5*) and in more detail by Swift (*4*). The dimensions of the bodies are given on Table 1.

A standard method for obtaining calibration data was carried out. First, values of β were determined for liquids (*n*-hexane to *n*-decane) from 20° to 100°C. at atmospheric pressure. The flow in the viscometer was laminar during these determinations. It was therefore possible to determine the variation of β with temperature without difficulty. If one assumes that β varied linearly with temperature, the temperature coefficient α of the equation

$$\beta = \beta_0(1+\alpha t) \quad (9)$$

was computed by the method of least squares.

The floats were then calibrated with gases. With gases under pressure the density-viscosity ratio was high enough to give turbulent flow in most cases. Thus the effect of turbulence on the viscometer constant could be determined.

The effect of pressure on β was not determined for the falling bodies, except in the case of MgSLO-309. For all other floats it was impossible to separate the effect of pressure on β from the effect of turbulence. Since the linear effect of pressure was determined to be only 3% maximum at 1,000 lb./sq. in absolute for MgSLO-309 (*5*) and the theoretical analysis showed the effect would be even less for the other, smaller diameter bodies, it was deemed unwise to use some approximate correction method for the other floats, for example, pressurizing *n*-heptane and assuming pressure had no effect on viscosity.

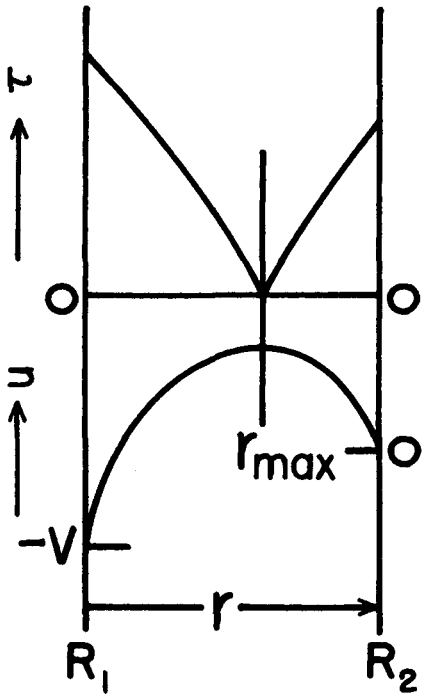

Fig. 1. Laminar flow profile and shear diagram between tube and body.

These data were first correlated on a plot of β_0 vs. $\rho/\mu\theta$, a dimensional group proportional to the Reynolds number. Sage and Lacey (*3*) presented their calibration data in this manner, although they did not consider effects of temperature and pressure on the viscometer constant. The type of plot obtained is shown in Figure 2. The value of β_0 is characteristically constant in the laminar flow region and decreases continuously in the turbulent region at higher values of $\rho/\mu\theta$.

CONSIDERATION OF VARIABLES

Effects of temperature and pressure

Using values of the linear coefficient of thermal expansion, Young's modulus, and Poisson's ratio for Pyrex glass and magnesium one could calculate values of β_{1sf} as a function of temperature and pressure using an IBM 650 digital computer. Although changes in β_{1sf} with temperature and pressure are not exactly linear and independent, β_{1sf} may be accurately reproduced by an equation of the form

$$\beta_{1sf} = \beta_{1sf(0,0)}(1+\alpha t+\gamma P) \quad (10)$$

Values of the temperature and pressure coefficients predicted by Equation (10) for β_{1sf} are compared with experimental coefficients for β in Table 2.

Excellent agreement between experimental and predicted temperature coefficients for the magnesium floats was found. The predicted temperature coefficients do not agree with the experimental values for the glass floats. Probable causes for disagreement are:

1. The steel body elevating device in the glass floats increases the thermal expansion.
2. The wall thickness of the glass floats varies with length.
3. The outside diameter of the cylindrical length of the glass floats varies.

For MgSLO-309, the only body for which an experimental pressure coefficient could be determined, the predicted pressure coefficient was slightly more than twice the experimental value. The steel machine screws in the magnesium bodies contributed to this disagreement. In any case both the predicted and experimental effects of pressure are small.

Effects of turbulent, contraction, expansion, and imperfection losses

Experimental values of the viscometer constant are compared with values predicted from Equation (8) for the

Table 1. Dimensions of the Viscometer Bodies and Tube

Distances between fiducial marks = 1.75 in.
Viscometer tube diameter = 0.3149 in.

Body code	Body diameter, in.	Lug diameter, in.	Over-all length, in.	Length of cylindrical section, in.	Volume equivalent length, in.	Body density, g./cc.
GCL-301	0.3010	0.312	3.5	2.9	3.03	1.437
GCLO-304	0.3038	0.312	1.9	1.6	1.72	1.612
MgSLO-303	0.3030	0.312	1.50	1.50	1.50	1.963
MgSLO-305	0.3050	0.312	1.25	1.25	1.25	1.991
MgSLO-307	0.3070	0.312	1.25	1.25	1.25	1.982
MgSLO-309	0.3090	0.312	1.25	1.25	1.25	1.990

Table 2. Experimental Results and Comparisons with Predicted Values

	Coefficients of temperature, α (10^4), °C.$^{-1}$		Coefficients of pressure, γ (10^4), (lb./sq. in abs.)$^{-1}$		Viscometer constant, β(10^5), sq. cm./sec.^{2}, at 20°C. and 1 atm.		critical N_{Re}	Errors in β/β_{1sf} as a function of N_{Re} laminar region, % error*	turbulent region, Ave. % error
	exp.	pred.	exp.	pred.	exp.	pred.			
GCL-301	2.88	0.0655	—	4.17	44.29	54.4	1.0	0.35	1.40
GCLO-304	5.28	0.0632	—	5.38	23.17	27.8	1.0	1.83	0.78
MgSLO-303	—16.7	-16.9	—	3.14	22.97	32.3	0.4	0.45	0.72
MgSLO-305	—19.3	-19.9	—	3.74	13.15	18.6	0.25	0.36	0.18
MgSLO-307	—24.8	-24.7	—	4.79	6.375	9.42	0.13	0.31	1.80
MgSLO-309	—32.0	-33.2	2.84	6.50	2.393	3.77	—	0.99	

* Computed at 98% statistical level.

six bodies studied in Table 2. Although agreement is sufficient to permit practical design predictions of the viscometer constant, the experimental values are consistently lower than those predicted owing to contraction, expansion, and imperfection losses.

Since these effects and the effect of turbulence cannot be treated mathematically, dimensional analysis was used to develop a correlation including these effects. Thus,

$$\phi_1 (F_g,\rho,v,\mu,g_c,D_e,d,1,1',---)=0 \quad (11)$$

Dimensional analysis yields

$$f=\frac{4F_g g_c D_e}{\pi d^2 \rho v^2 l}$$

$$=\phi_2\left(N_{Re},\frac{d}{D_e},\frac{1}{D_e},\frac{1'}{D_e},---\right) \quad (12)$$

When only laminar flow occurs, substitution of Equation (7) into Equation (12) gives

$$f=\frac{16}{N_{Re}} \quad (13)$$

On Figure 3 the data for MgSLO-305 are plotted to illustrate the friction factor as a function of the Reynolds number. Although the shape factors change slightly with temperature and pressure, the effect of these quantities is small for any given body. At low values of the Reynolds number the slope of the line on Figure 3 is constant and equal to minus one, indicating all appreciable frictional effects are laminar. At higher values of the Reynolds number turbulent effects become appreciable. The difference between the curve for MgSLO-305 data and the lower line, which is based on laminar flow only, is due to the effects of turbulent, contraction, expansion, and imperfection losses.

CALIBRATION PLOTS

Since the viscosity occurs only in the Reynolds number, a friction factor plot such as Figure 3 could be used directly as a working plot to determine unknown viscosities. Because of the logarithmic coordinates however it is difficult to read this plot accurately.

Relation between β and β_{1sf}

The use of β or the ratio β/β_{1sf} gives a more sensitive representation of calibration data. Since

$$fN_{Re}=\frac{16\,\beta_{1sf}}{\beta} \quad (14)$$

from Equation (12)

$$\frac{\beta}{\beta_{1sf}}=\phi_3\left(N_{Re},\frac{d}{D_e},\frac{1}{D_e},\frac{1'}{D_e},---\right) \quad (15)$$

The plots of β/β_{1sf} vs. the Reynolds number were constructed and were of the same nature as the β_o vs. $\rho/\mu\theta$ plots represented on Figure 2. For these plots β_{1sf} and D_e in the Reynolds number were computed as a function of temperature and pressure with the mechanical properties of glass and magnesium previously mentioned. Again the shape factors appear to have little effect.

Comparison of calibration plots

The errors for the β/β_{1sf} vs. N_{Re} plots are given on Table 2. The errors for the β_o vs. $\rho/\mu\theta$ plots were in general less than or nearly the same as the errors for the β/β_{1sf} vs. N_{Re} plots. Al-

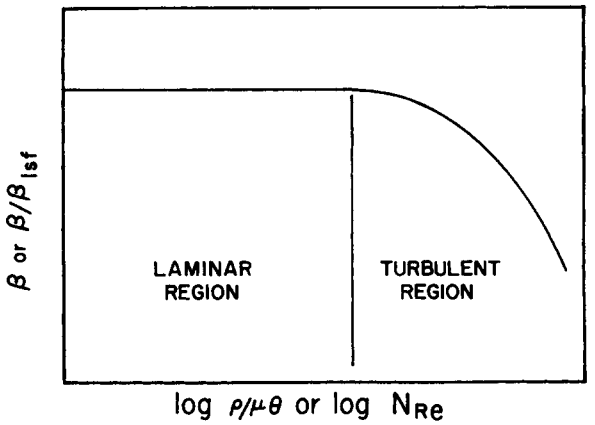

Fig. 2. Characteristic plot of β_o vs. $\rho/\mu\theta$ and β/β_{1sf} vs. N_{Re}.

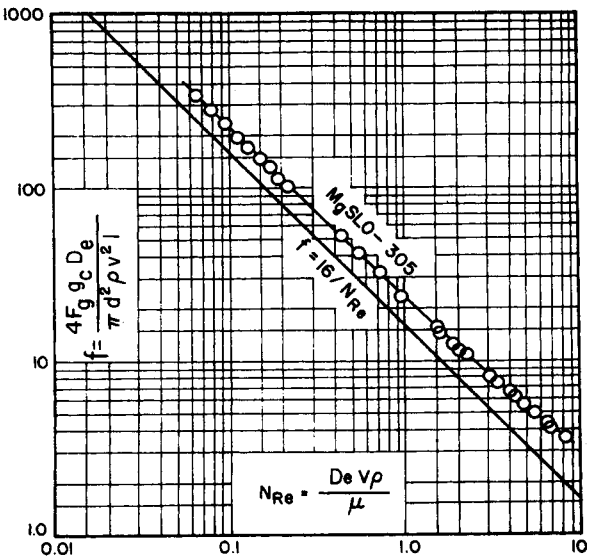

Fig. 3. Friction factor vs. the Reynolds number for body MgSLO-305.

though the β/β_{1sf} vs. N_{Re} plot is more theoretically complete, there is no apparent advantage in the use of this plot. When more accurate measurements of the dimensions, particularly D and d, become possible, the β/β_{1sf} vs. N_{Re} plot will be more advantageous to use, since this type of presentation describes the geometry of the viscometer.

DESIGN OF VISCOMETERS

Falling cylinder viscometers can be designed by using Equation (8) for specified ranges of viscosity and fall time with a higher accuracy than any present method. Accuracy is improved when the correction factor for nonskin friction losses, $(\beta/\beta_{1sf})_{laminar}$, is used in conjunction with Equation (8). Longer, more streamlined floats and smaller values of d/D would give values of the correction factor approaching unity. Below a Reynolds number of 0.1 all frictional effects may be assumed to be laminar.

It should be emphasized that any present design method will not eliminate experimental calibration. The falling cylinder viscometer cannot be used as an absolute instrument until improvements in physical dimension measuring techniques have been made. In this investigation it was found that viscometer dimensions would have to be uniform and measured within one part of 10^6 in order to accurately compute β_{1sf} to four significant figures.

Two approaches are possible to further improve the design methods presented here. First, the float might be long and streamlined so that even at high values of d/D the value of β/β_{1sf} approaches unity in the laminar region. In this case β/β_{1sf} would be a function of N_{Re} only, and it would not be necessary to consider the shape factors. Also, the lugs or projections could be mounted above and below the main body of the float; then the velocity past the projections would be lower, thereby reducing the imperfection friction losses. Second, with Equation (15) used as a basis a series of different bodies could be studied to evaluate the effect of the shape factors on β/β_{1sf}. The goal of this study would be a general design relation applicable for both laminar and turbulent flow for a family of bodies that are completely specified by the dimensions, D, D_e, and 1. For purposes of design the present ± 0.0001-in. accuracy in measurement of dimensions is sufficient. Much better accuracy will be necessary before a falling cylinder viscometer constant can be described completely by theory.

However other viscometers which are claimed to be absolute, for example, capillary, rotational, and vibrational, require some calibration to include effects of nonuniform dimensions and the possibility of turbulence. A good example of the sensitivity of the capillary viscometer to measurements and nonuniform construction is given by the work of Swindells, Coe, and Godfrey (8) in the redetermination of the absolute viscosity of water.

CONCLUSIONS

1. A theoretical analysis for a falling cylinder viscometer was developed, based on flow in an annulus. The viscometer constants calculated by this theory agreed with experimental values sufficiently well to permit design predictions.

2. Effects of temperature on the viscometer constant may be satisfactorily predicted from the theoretical analysis.

3. The β/β_{1sf} vs. N_{Re} plot or the β_o vs. $\rho/\mu\theta$ plot can be used to present experimental calibration data with comparable accuracy. Since the β/β_{1sf} vs. N_{Re} plot includes the dimensions of the viscometer, it is particularly suited for design applications.

ACKNOWLEDGMENT

The authors wish to thank the Phillips Petroleum Company for financial support and for providing the hydrocarbons used in this work.

NOTATION

D = diameter of the viscometer tube, cm.

D_e = $d\sqrt{\ln(D/d) - (D^2-d^2)/(D^2+d^2)}$ = equivalent diameter of the viscometer tube-body annulus, cm.

d = diameter of the cylindrical section of the viscometer body, cm.

F_g = force of gravity on the falling body, g-force

f = friction factor, dimensionless

g = local acceleration of gravity, cm./sec.^{2}

g_c = universal gravitational constant, g-mass-cm./g.-force-sec.^{2}

l = length of the cylindrical section of the viscometer body, cm.

l' = $V/\pi R_1^2$ = volume equivalent length of the viscometer body, cm.

N_{Re} = $D_e v\rho/\mu$ = Reynolds number, dimensionless

P = pressure in the viscometer, lb./sq. in. abs.

ΔP_{1sf} = pressure drop for laminar flow friction, g-force/sq. cm.

Q = volumetric flow rate of fluid, cc./sec.

R_2 = radius of the viscometer tube, cm.

R_1 = radius of the cylindrical section of the viscometer body, cm.

r = local radius in the annulus, cm.

r_{max} = local radius of maximum point velocity, that is where $du/dr = 0$ and $\tau = 0$, cm.

s = distance between fiducial marks, cm.

t = temperature of the viscometer, °C.

u = point fluid velocity, cm./sec.

du/dr = point velocity gradient, sec.$^{-1}$

V = volume of the viscometer body, cc.

$v=s/\theta$ = terminal velocity of the viscometer body, cm./sec.

Greek Letters

α = temperature coefficient of the viscometer constant, °C.$^{-1}$

β = viscometer constant, sq. cm./sec.^{2}

β_o = viscometer constant corrected to 0°C. and zero pressure, sq. cm./sec.^{2}

β_{1sf} = viscometer constant based on laminar flow only, sq. cm./sec.^{2}

$\beta_{1sf(0,0)}$ = β_{1sf} at 0°C. and zero pressure, sq. cm./sec.^{2}

$(\beta/\beta_{1sf})_{laminar}$ = correction factor for nonskin friction losses = constant ratio of β/β_{1sf} in the laminar region

γ = pressure coefficient of the viscometer constant, (lb./sq. in. abs.)$^{-1}$

θ = fall time interval, sec.

μ = absolute viscosity, poise or g.-mass/cm.-sec.

ρ = fluid density, g.-mass/cc.

$\rho/\mu\theta$ = nongeometric Reynolds group, (sq. cm.)$^{-1}$

σ = viscometer body density, g.-mass/cc.

τ = shear force parallel to and opposing flow, g.-force/sq. cm.

ϕ = general function

LITERATURE CITED

1. Barr, Guy, "A Monograph of Viscometry," Humphrey Milford, London (1931).
2. Hubbard, R. M., and G. G. Brown, *Ind. Eng. Chem., Anal. Ed.*, **15**, 212 (1943).
3. Sage, B. H., and W. N. Lacey, *Ind. Eng. Chem.*, **30**, 829 (1938).
4. Swift, G. W., Ph.D. Thesis, Univ. Kansas, Lawrence, Kansas (1959).
5. ———, John Lohrenz, and Fred Kurata, *A.I.Ch.E. Journal*, **6**, 415 (1960).
6. Swindells, J. F., J. R. Coe, Jr., and T. B. Godfrey, *J. Res. Nat. Bur. Stan.*, **48**, 1 (1952).

Manuscript received June 5, 1959; revision received February 22, 1960; paper accepted February 23, 1960. Paper presented at A.I.Ch.E. St. Paul meeting.